

Waste tailing Particle Electrode enables enhance electrochemical degradation for sulfamethoxazole

Jiaqi Bu^a, Hongru Jiang^a, Tianhao Li^a, Chengyun Zhou^{b*}, Shian Zhong^{a*},

^aCollege of Chemistry and Chemical Engineering, Central South University, Changsha, 410083, PR China.

^bCollege of Environmental Science and Engineering, Hunan University and Key Laboratory of Environmental Biology and Pollution Control (Hunan University), Ministry of Education, Changsha 410082, P.R. China

* Corresponding author, Email: zhongshiancsu@163.com; (S.A. Zhong); zhouchengyun@hnu.edu.cn; (C.Y. Zhou);

Text S1. The Analytical Methodologies

The physical morphology and element composition of the plate surface was analyzed by (SEM; MIRA 3 LMU; Czech Republic), (EDS; Oxford X-Max20; Czech Republic), and Zeta potential (NanoPlus). X-ray polycrystalline powder diffractometer (XRD; Ultima IV; Japan) and X-ray photoelectron spectroscopy (XPS; ESCALAB250Xi; America) were used to analyze the crystal structure and valence composition of the metal on the surface of the electrode. The electrochemical workstation (EW; CHI660E; Shanghai, China) was used to analyze various electrocatalytic activities and chlorine evolution performance of the electrode. electron paramagnetic resonance (EPR) was used to confirm the generation of free radicals. UV spectrophotometer (UV-Vis, Cary 8454 UV-Vis, Shanghai, China), Total organic

carbon analyzer (TOC, TOC-L, Shimadzu Corporation), and High-performance liquid chromatography (HPLC, LC-20A, Japan) were used to analyze the removal efficiency of SMZ. The degradation mechanism was analyzed by Triple quadrupole liquid chromatography-mass spectrometry (LC-MS, 1260-6460, Agilent). Toxicity Estimation Software Tool software was used to analyze the toxicology of water quality before and after degradation.

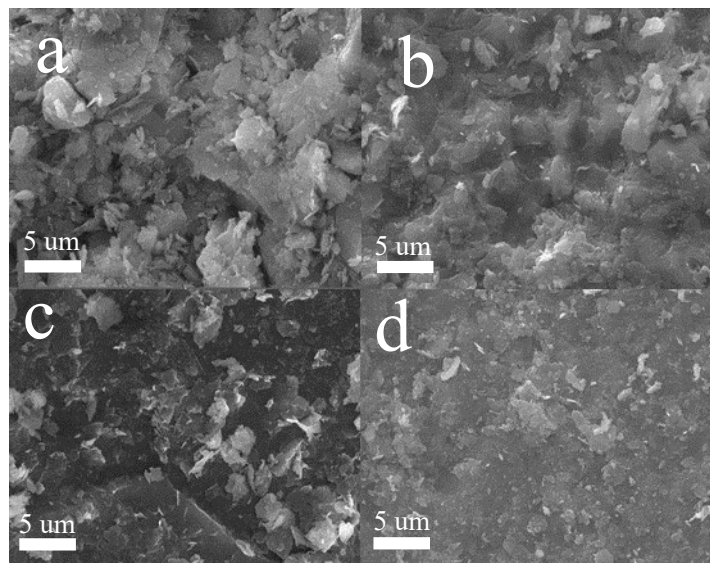


Fig. S1. SEM images of LZT-SO calcined at 350 °C (a), 450 °C (b), 550 °C (c), and 650 °C (d), respectively.

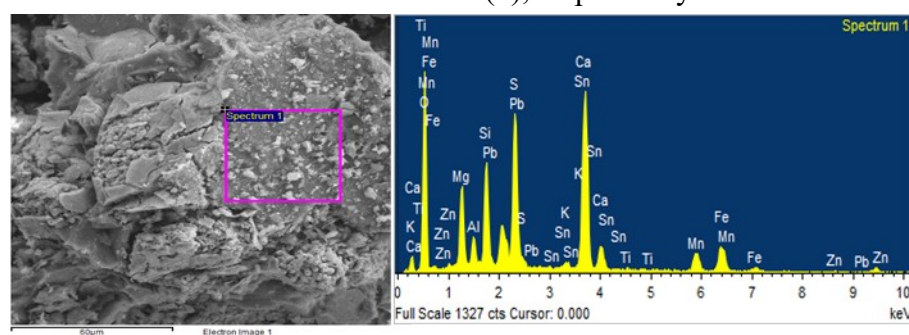


Fig. S2. The SEM and EDS of LZT.

Table S1. The element proportion of LZT.

| Element | Weight% | Atomic% |
|---------|---------|---------|
| O K | 50.34 | 69.62 |
| Mg K | 5.27 | 4.79 |
| Al K | 1.57 | 1.29 |
| Si K | 5.52 | 4.35 |
| S K | 9.61 | 6.63 |

| | | |
|--------|--------|--------|
| K K | 0.57 | 0.32 |
| Ca K | 15.86 | 8.76 |
| Ti K | 0.06 | 0.03 |
| Mn K | 3.92 | 1.58 |
| Fe K | 6.21 | 2.46 |
| Zn K | 0.09 | 0.03 |
| Sn L | 0.36 | 0.07 |
| Pb M | 0.62 | 0.07 |
| Totals | 100.00 | 100.00 |

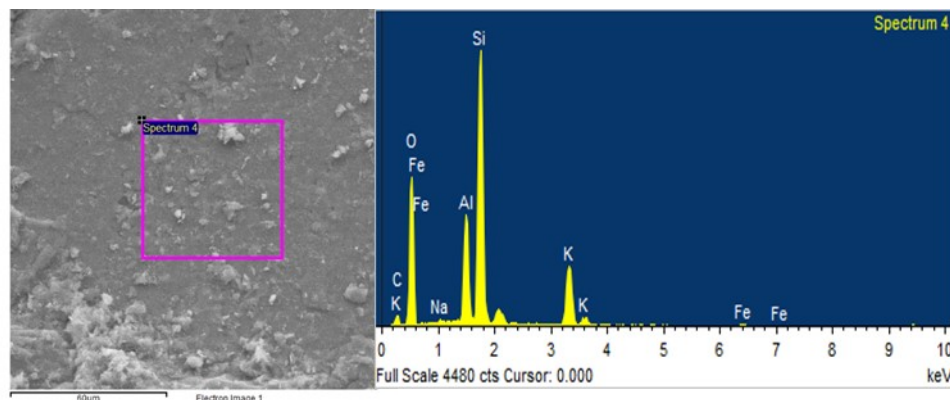


Fig. S3. The SEM and EDS of SO.

Table S2. The element proportion of SO.

| Element | Weight% | Atomic% |
|---------|---------|---------|
| C K | 7.44 | 11.83 |
| O K | 51.92 | 61.99 |
| Na K | 0.33 | 0.28 |
| Al K | 7.81 | 5.53 |
| Si K | 23.84 | 16.22 |
| K K | 8.19 | 4.00 |
| Fe K | 0.47 | 0.16 |
| Totals | 100.00 | 100.00 |

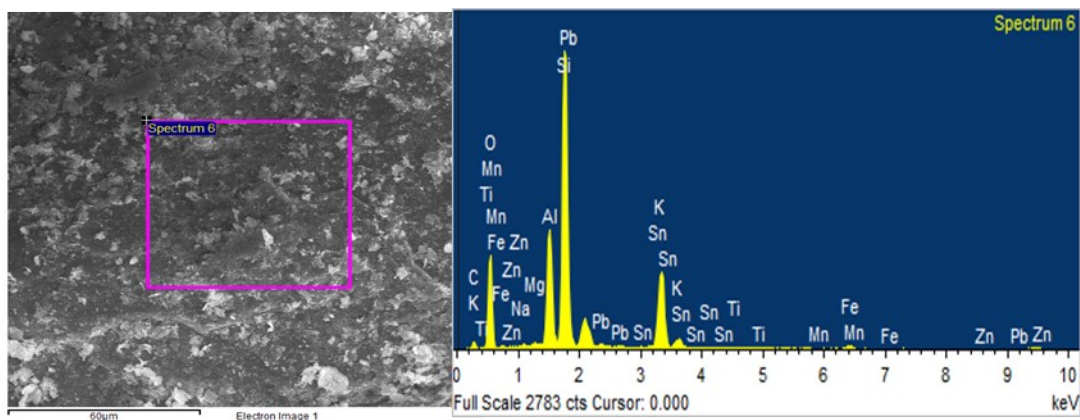


Fig. S4. The SEM and EDS of LZT-SO.

Table S3. The element proportion of LZT-SO.

| Element | Weight% | Atomic% |
|---------|---------|---------|
| C K | 6.32 | 10.85 |
| O K | 53.54 | 63.35 |
| Na K | 0.37 | 0.31 |
| Mg K | 0.60 | 0.34 |
| Al K | 6.02 | 4.24 |
| Si K | 27.83 | 18.81 |
| Sn K | 0.17 | 0.11 |
| K K | 1.02 | 0.50 |
| Ca K | 0.14 | 0.07 |
| Ti K | 0.21 | 0.08 |
| Mn K | 0.59 | 0.22 |
| Fe K | 2.82 | 1.02 |
| Zn K | 0.12 | 0.05 |
| Pb M | 0.21 | 0.09 |
| Totals | 100.00 | 100.00 |

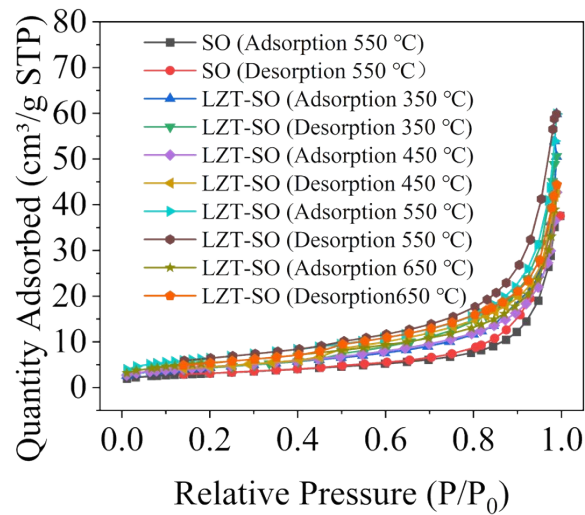


Fig. S5. Nitrogen adsorption and desorption isotherms of LZT-SO and SO

calcined at no temperature.

Table S4 Pore structure parameters of LZT-SO and SO.

| Samples | Surface Area (m ² /g) | Pore Volume (cm ³ /g) | Average Pore Size (nm) |
|---------|-------------------------------------|-------------------------------------|---------------------------|
| SO | 11.1604 | 0.05741 | 20.5749 |
| LZT-SO | 23.1724 | 0.09258 | 15.9817 |

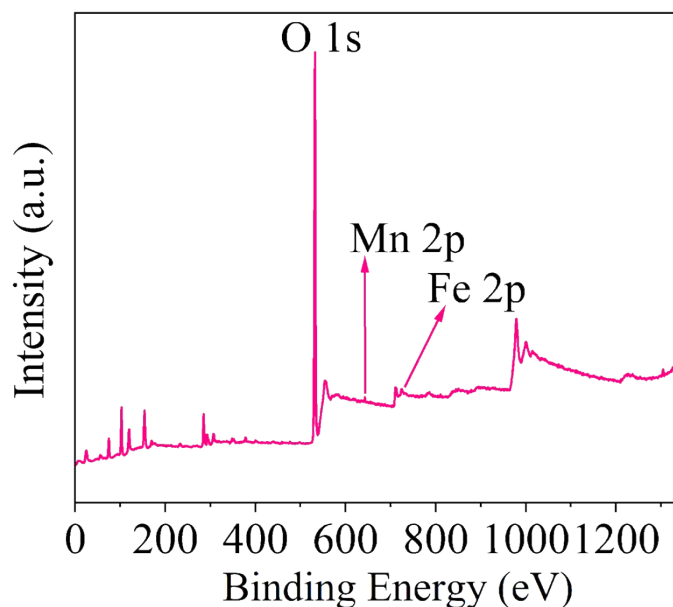


Fig. S6. The XPS total spectrum of LZT-SO.

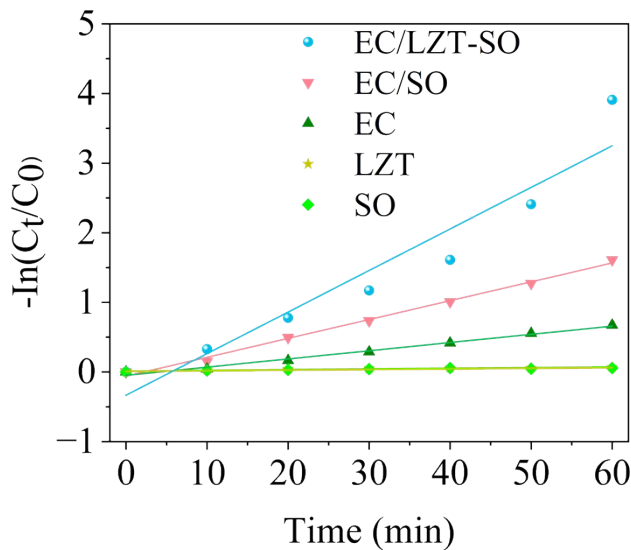


Fig. S7. Linear fittings of the pseudo-first-order model.

Text S4. The specific operating parameters of the electrochemical workstation

The ITO electrode was ultrasonically cleaned in acetone, 1 mol L⁻¹ sodium hydroxide solution, and deionized water for 15 min, dried with nitrogen, and then dried at 120 °C for 2 h. Weigh 8 mg of particle electrode (LZT-SO) material, disperse it in 4 mL of ultrapure water, ultrasonic for 30 min, evenly drop 30 uL suspension on ITO electrode in a fixed area, and dry it at room temperature. Then, start the test.

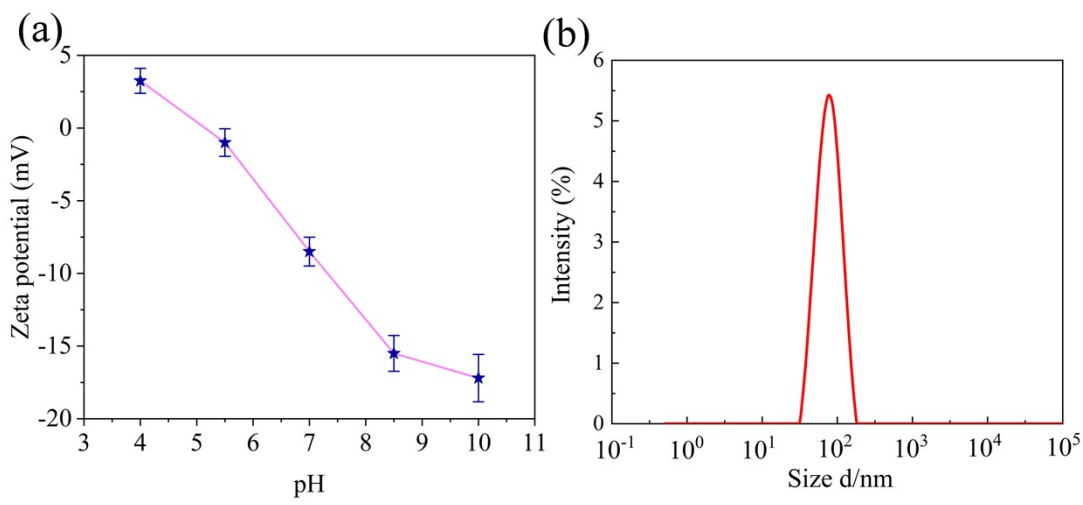


Fig. S8. The zeta potentiometer (a) and nanoparticle size (b) of LZT-SO.

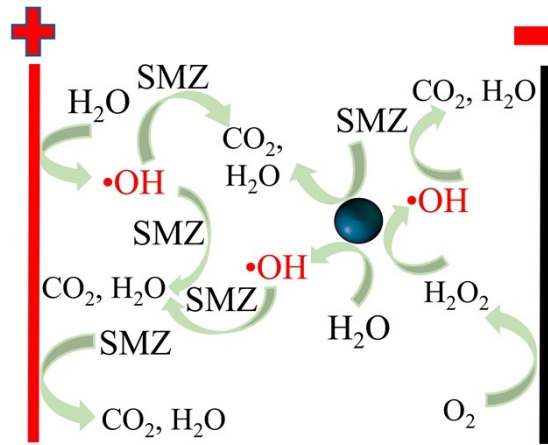


Fig. S9. The possible degradation mechanism of SMZ.

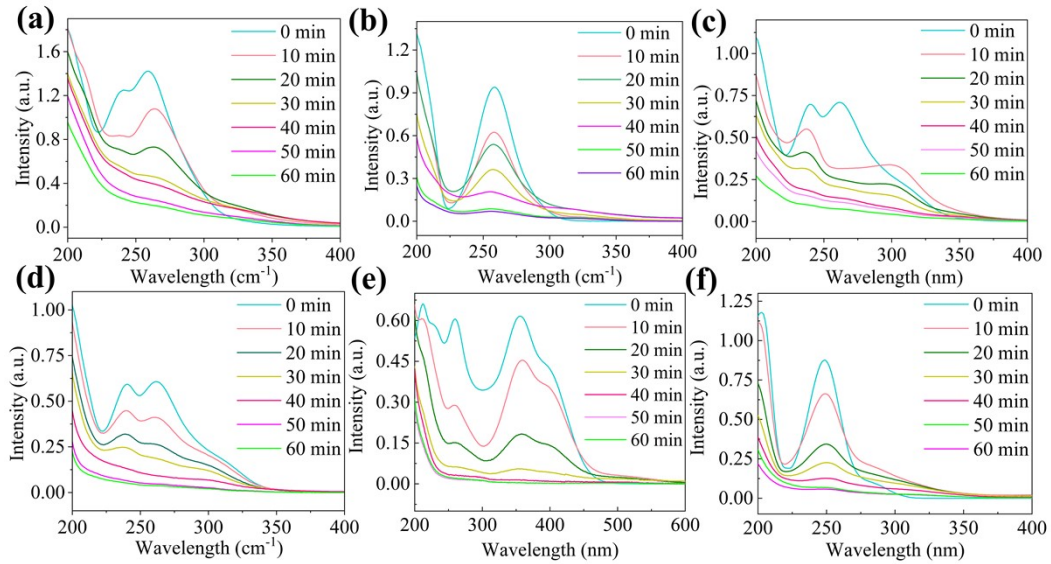


Fig. S10. UV absorption spectra of SMZ (a), SA (b), SAZ (c), SMA (d), 2,4-dinitrophenol (e), and 4-aminobenzenesulfonic acid (f) before and after degradation (pH=6.02, pate spacing=4 cm, aeration flow rate=12 L/h, voltage=10 V, Na_2SO_4 dose=0.050 mmol, the dose of LZT-SO=35.02 g, $[\text{SMZ}]_0=10.02 \text{ mg/L}$, the degradation time=70 min).

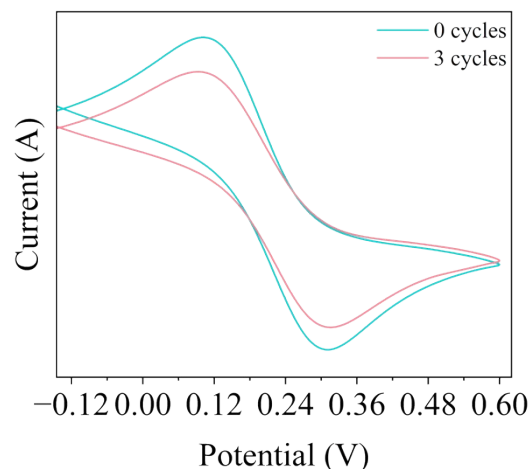


Fig. S11. Cyclic voltammetry curve of 0 cycle and 3 cycles.

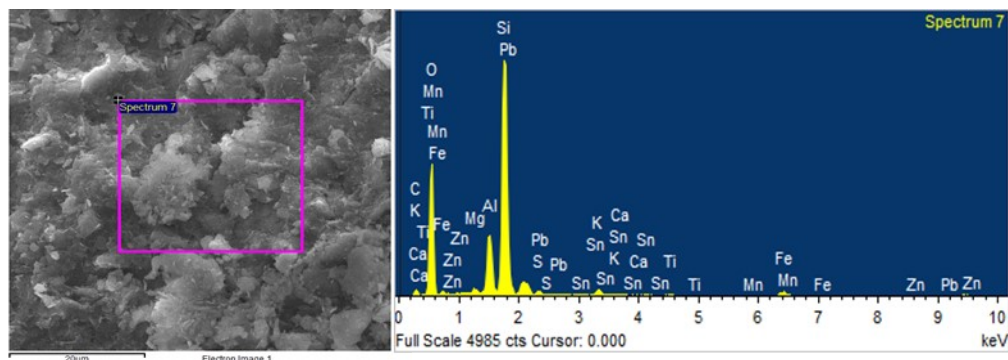


Fig. S12. The SEM and EDS of LZT-SO after three cycles.

Table S5. The element proportion of waste coal cinder after three cycles

| Element | Weight% | Atomic% |
|---------|---------|---------|
| C K | 6.51 | 10.93 |
| O K | 53.87 | 63.43 |
| Na K | 0.39 | 0.32 |
| Mg K | 0.58 | 0.33 |
| Al K | 6.06 | 4.26 |
| Si K | 27.84 | 18.8 |
| Sn K | 0.15 | 0.1 |
| K K | 1.01 | 0.5 |
| Ca K | 0.15 | 0.07 |
| Ti K | 0.18 | 0.06 |
| Mn K | 0.5 | 0.17 |
| Fe K | 2.52 | 0.92 |
| Zn K | 0.09 | 0.04 |
| Pb M | 0.15 | 0.07 |
| Totals | 100.00 | 100.00 |

Table S6. The mass loss of LZT-SO after three cycles

| Cycles | Mass loss (%) |
|--------|---------------|
| 0 | 0 |
| 1 | 1.56 |
| 2 | 3.21 |
| 3 | 5.46 |

Table S7 Comparison of different methods for removal antibacterial.

| Method | Contaminants | Concentratio n | Time (h) | Removal efficiency (%) | pH | Ref |
|----------------|------------------|-------------------|-------------|------------------------------|-----|--------------------|
| Adsorption | Sulfanilamide | 10 mg/L | 4 | 86.77 | 6 | (Sun et al., 2022) |
| Photocatalytic | Sulfamethoxazole | 20 mg/L | 2/3 | 89.02 | 7.5 | (Paragas et |

| | | | | | | |
|--|------------------|-----------|-----|--------------|----------|--|
| Sonocatalytic | Sulfamethoxazole | 10 µM /L | 1 | 95 | 7 | al., 2018) (Al-Hamadani et al., 2016) |
| Ozone Oxidative | Sulfamethoxazole | 1000 µg/L | 0.5 | 96-98 | 3.5 | (Garoma et al., 2010) |
| Fenton Oxidative | Sulfamethoxazole | 20 mg/L | 2/3 | 87.8 | 6.5 | (Liu et al., 2021) |
| Peroxide activation | Sulfamethoxazole | 10 mg/Kg | 36 | 95.8 | 6 | (Amina et al., 2022) |
| Biological oxidation | Sulfamethoxazole | 52 µg/L | 168 | 47.86 ± 2.35 | 8.4 | (Rodrigues et al., 2020) |
| Three-dimensional electrocatalytic oxidation | Sulfamethoxazole | 10 mg/L | 1 | 100.00 | 6.0 2 | This work |

Amina, Abbas, Q., Shakoor, A., Naushad, M., Yousaf, B., 2022. In-situ oxidative degradation of sulfamethoxazole by calcium peroxide/persulfate dual oxidant system in water and soil. Process. Saf. Environ. 164, 696-705. <https://doi.org/10.1016/j.psep.2022.06.052>.

Al-Hamadani, Y.A.J., Chu, K.H., Flora, J.R.V., Kim, D.H., Jang, M., Sohn, J., Joo, W., Yoon, Y., 2016. Sonocatalytical degradation enhancement for ibuprofen and sulfamethoxazole in the presence of glass beads and single-walled carbon nanotubes. 32, 440-448. <https://doi.org/10.1016/j.ultsonch.2016.03.030>.

Garoma, T., Umamaheshwar, S.K., Mumper, A., 2010. Removal of sulfadiazine, sulfamethizole, sulfamethoxazole, and sulfathiazole from aqueous solution by ozonation. Chemosphere. 79, 814-820. <https://doi.org/10.1016/j.chemosphere.2010.02.060>.

Liu, Y., Yang, Z., Wang, J.L., 2021. Fenton-like degradation of sulfamethoxazole in Cu⁰/Zn⁰-air system over a broad pH range: Performance, kinetics and mechanism. Chem. Eng. J. 403, 126320. <https://doi.org/10.1016/j.cej.2020.126320>.

Rodrigues, D.A.D., da Cunha, C.C.R.F., Freitas, M.G., de Barros, A.L.C., Castro, P.B.N.E., Pereira, A.R., Silva, S.D., Santiago, A.D., Afonso, R.J.D.F., 2020. Biodegradation of sulfamethoxazole by microalgae-bacteria consortium in wastewater treatment plant effluents. Sci.Total. Environ. 749, 141441. <https://doi.org/10.1016/j.scitotenv.2020.141441>.

Sun, Y., Bian, J.M., Zhu, Q., 2022. Sulfamethoxazole removal of adsorption by carbon – Doped boron nitride in water. J. Mol. Liq. 349, 118216. <https://doi.org/10.1016/j.molliq.2021.118216>.

Paragas, L.K.B., de Luna, M.D.G., Doong, R.A., 2018. Rapid removal of sulfamethoxazole from simulated water matrix by visible-light responsive iodine

and potassium co-doped graphitic carbon nitride photocatalysts. Chemosphere. 210, 1099-1107. <https://doi.org/10.1016/j.chemosphere.2018.07.109>.

Table S8 Degradation process parameters and cost.

| Factor | Parameter | SMZ removal efficiency (%) | Power consumption (kW·h) |
|--|-----------|----------------------------|--------------------------|
| pH | 4.01 | 90.11 | 1.70 |
| | 6.02 | 100.00 | 1.51 |
| | 7.02 | 96.02 | 1.55 |
| | 7.99 | 98.01 | 1.61 |
| | 9.98 | 84.02 | 1.74 |
| Na_2SO_4 dosage (mmol) | 0.00 | 9.23 | 0.11 |
| | 0.25 | 89.11 | 0.84 |
| | 0.40 | 93.52 | 1.28 |
| | 0.50 | 100.00 | 1.51 |
| | 0.60 | 100.00 | 1.68 |
| Voltage (V) | 0.70 | 100.00 | 1.82 |
| | 6 | 94.01 | 0.96 |
| | 8 | 98.01 | 1.39 |
| | 10 | 100.00 | 1.51 |
| | 12 | 100.00 | 1.70 |
| Aeration flow rate (L/h) | 14 | 100.00 | 1.86 |
| | 0 | 83.91 | 1.61 |
| | 8 | 95.71 | 1.58 |
| | 10 | 97.71 | 1.59 |
| | 12 | 100.00 | 1.51 |
| Groove spacing (cm) | 14 | 92.40 | 1.42 |
| | 4 | 100.00 | 1.51 |
| | 5 | 95.02 | 1.22 |
| | 6 | 91.12 | 0.81 |

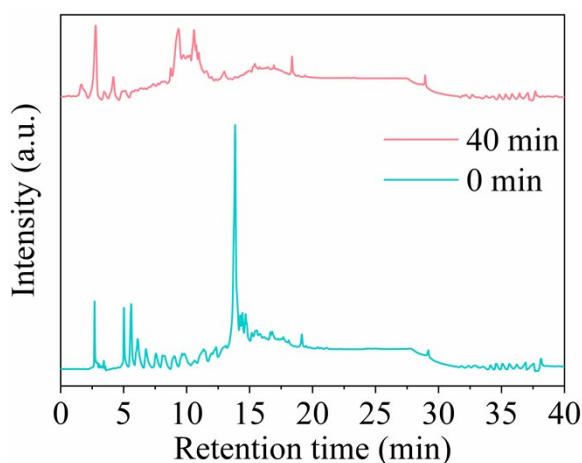


Fig. S13. The total ion chromatography spectra of SMZ before and after degradation.

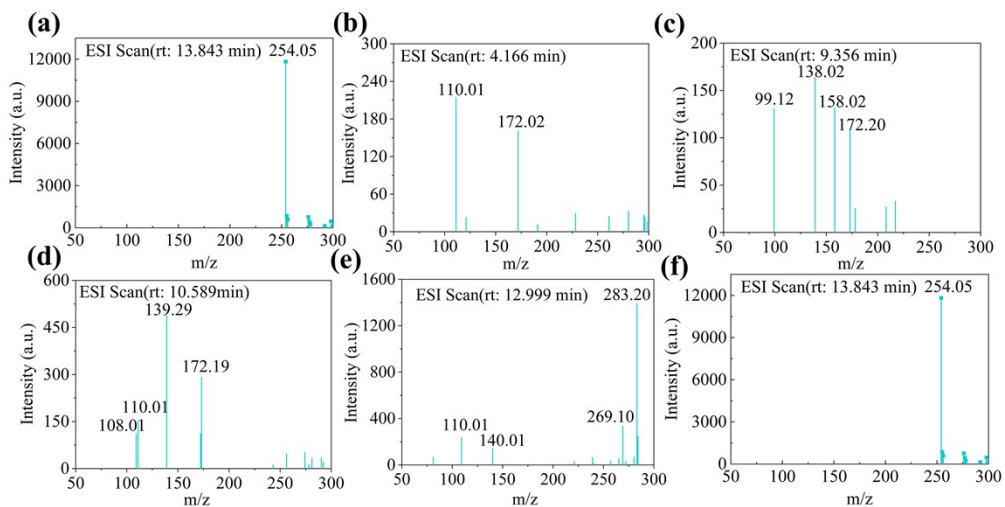


Fig. S14. The mass spectra of SMZ before (a) and after degradation (b-f).

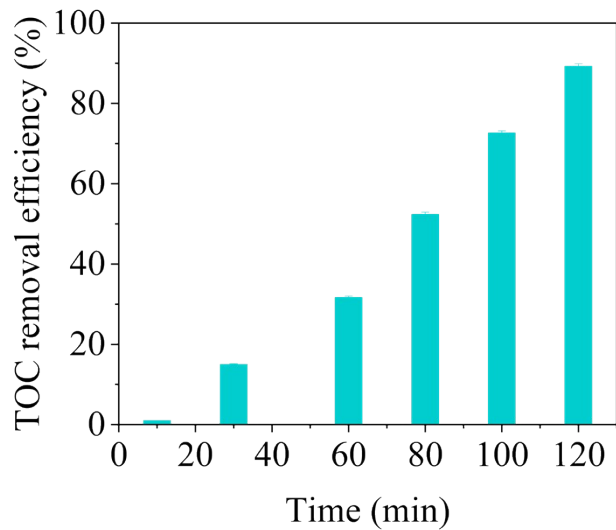
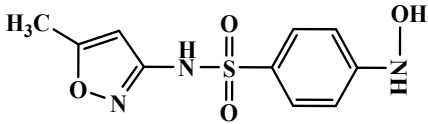
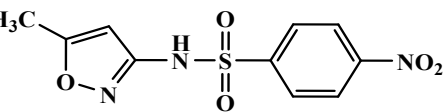
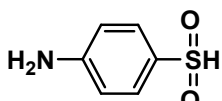
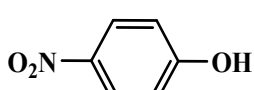
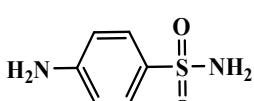
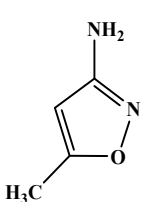
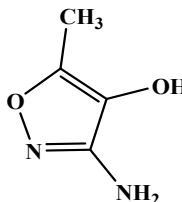


Fig. S15. The TOC removal efficiency of SMZ before and after degradation (pH=6.02, plate spacing=4 cm, aeration flow rate=12 L/h, voltage=10 V, Na₂SO₄ dose=0.050 mmol, the dose of LZT-SO=35.02 g, [SMZ]₀=10.02 mg/L).

Table S9. The structural information of the possible intermediate products.

| Compound | Molecular structure | Mass/charge ratio (m/z) |
|----------|--|-------------------------|
| SMZ | <chem>CN1C=CC2=C1ON=C2Nc3ccccc3S(=O)(=O)N4Cc5ccccc5N4</chem> | 254.05 |

| | | |
|-----|---|--------|
| P1 |  | 269.1 |
| P2 |  | 283.2 |
| P3 |  | 110.1 |
| P4 |  | 108.1 |
| P5 |  | 158.02 |
| P6 |  | 138.1 |
| P7 |  | 139.29 |
| P8 |  | 172.2 |
| P9 |  | 99.12 |
| P10 |  | 140.01 |